

Layer growth of methane on MgO: An adsorption isotherm study

Andrea Freitag and J. Z. Larese

Chemistry Department, Brookhaven National Laboratory, Upton, New York 11973-5000

(Received 14 April 2000)

The layering properties of methane on MgO (100) were measured between 70 K and 96 K using high-resolution adsorption isotherms. The results demonstrate that at least five layers can form. Phase transitions for the different layers were identified by monitoring the changes in the isothermal compressibility of a particular layer as a function of chemical potential. A phase transition (melting) for the monolayer is observed at about 80 K, whereas layers 2 through 4 show a similar transition at about 85 K. The isosteric heat of adsorption was calculated as a function of coverage to gain insight into the growth process of the CH₄/MgO system. The thermodynamic quantities determined here are compared with published experimental values. Our data provide key information for defining current methane-MgO interaction potentials.

I. INTRODUCTION

Methane is an ideal choice for investigating the adsorption properties of substrates with different surface symmetry because the molecular symmetry and crystal symmetry of the bulk solid (i.e., cubic, closed packed) facilitates the formation of two-dimensional (2D) solids with either sixfold or fourfold symmetry depending on the structure of the adsorbing surface. Additionally, at high temperature methane exhibits classical adsorption behavior (e.g., translational diffusion and uniform layering) while at low temperatures it exhibits quantum behavior (e.g., rotational tunneling). Finally, the relative strengths of the adsorbate-adsorbate interactions versus those of the adsorbate-substrate should lead to interesting order-disorder and layering phenomena.

Significant theoretical and experimental progress has been made in understanding the adsorption properties of methane on a graphite basal plane composed of the well-known hexagonal network of carbon atoms. These studies examined the thermodynamic properties, monolayer and multilayer melting and structure, commensurate and incommensurate transitions, and orientational ordering and wetting. Bruch, Cole, and Zaremba's monograph¹ contains a good review and bibliography of these earlier studies.

We discuss here our thermodynamic characterization of the multilayer adsorption properties of CH₄ on the (100) surface of MgO using adsorption isotherms. MgO is an ionic crystal with a cubic, rock-salt structure. On the (100) surface, Mg and O atoms are distributed on a square lattice.

A body of knowledge exists on the behavior of thin CH₄ films (one-to-three layers thick) on MgO. However, there are fewer studies of adsorption on MgO because the preparation and handling of the sample is more challenging than it is for graphite (see e.g., Coulomb, Sullivan, and Vilches²) since the MgO surface tends to readily hydroxylize. Nevertheless, there is some information on the structure and translational dynamics of CH₄ monolayer and multilayers on an MgO substrate. For example, using neutron diffraction Coulomb *et al.*³ showed that at monolayer thickness CH₄ forms a $\sqrt{2} \times \sqrt{2}R45^\circ$ square solid on MgO at 50 K. Gay, Suzanne, and Coulomb examined the structure and dynamics of thin films of methane on MgO near the bulk triple point. They found

that the formation of solid multilayers is aided by the fact that the MgO (100) surface is a nearly perfect template for growing the (100) plane of bulk methane. We confirmed their findings using neutron diffraction.⁵ Gay, Suzanne, and Coulomb⁴ also reported that melting takes place near 80 K at monolayer coverage but that the melting temperature increases with increasing film thickness. Lakhlifi and Girardet⁶ have studied the CH₄/MgO system theoretically and predicted that near 80 K and at monolayer thickness the isosteric heat of adsorption should be about 160 meV. While much is known about the behavior of monolayer methane films on MgO some uncertainties remain. For example, on graphite, monolayer methane solid films form with the C_{3v} axis of the molecule perpendicular to the surface plane (the so-called tripod-down configuration). But, on MgO, the molecular orientation is debatable.⁷⁻⁹ New theoretical work on this topic^{10,11} was stimulated by high-resolution inelastic-neutron-scattering measurements by Larese,⁵ which characterize the low-temperature rotational dynamics of the CH₄/MgO system. Analysis of the neutron rotational tunneling spectra indicates that a C_{2v} orientation of the molecule provides the best fit of the monolayer data.

A very limited amount of thermodynamic data about the multilayer CH₄/MgO system was included in the studies cited above; however, there has been no comprehensive examination of the thermodynamics of methane on MgO adsorption. Some information on the thermodynamics was given by Coulomb, Sullivan, and Vilches² and by Madih.¹² They used adsorption isotherms to set a critical temperature for the monolayer at 80 ± 2 K with greater uncertainties on the transition temperatures for higher layers (i.e., for the second and third layer ≥ 87 K). We undertook this thermodynamic study as part of our ongoing investigations of layer-by-layer growth, surface melting, and the rotational dynamics of methane on MgO using inelastic-neutron-scattering techniques.^{5,13,14}

II. EXPERIMENTAL PROCEDURE

The MgO powder used in this study was prepared from magnesium vapors using, to our knowledge, a novel process¹⁵ (patent pending). Electron microscope examination

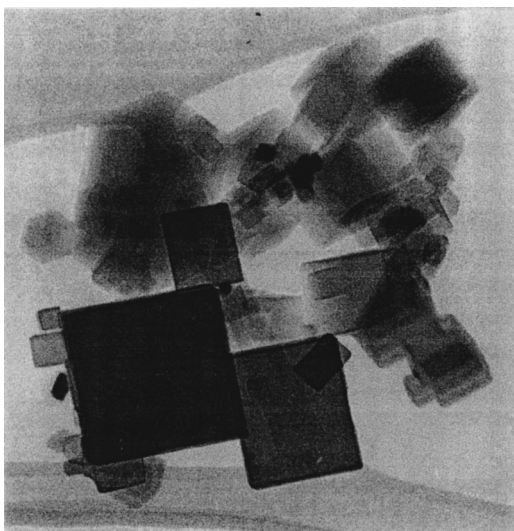


FIG. 1. Transmission electron micrograph of random MgO powders used in this paper. The largest cube is approximately 2000 Å on a side.

of these powders shows that they contain cubic particles (about 2500 Å cube edge, see Fig. 1) with a narrow distribution of particle size. Typically, the powders have a surface area of about 10 m²/g. The total amount of impurities in the MgO was no more than a few ppm. The MgO powder was heat treated *in vacuo* at 950 °C for about 36 h before use.

Approximately 0.5 g of the heat-treated MgO powder was loaded into an oxygen-free-high-conductivity copper cell and indium sealed inside a glove box filled with argon. Special care was taken to avoid exposing the samples to air since extended exposure to moisture hydroxylates the MgO surface. This is a significant problem with most MgO samples because most have a substantial number of oxygen vacancies, the primary surface defects for MgO (100). The sealed cell then was mounted on the second stage of a displax, closed-cycle helium cryostat. The dead space of the sample cell was measured as function of temperature using He gas. Its temperature was monitored during the experiments with two temperature sensors, one on the sample cell and the other on the second stage of the refrigerator. The accuracy of the temperature sensors was checked against the saturated vapor pressure of the methane gas.

Adsorption isotherms were measured volumetrically using an automated apparatus described elsewhere.¹⁶ The data from the isotherm measurements between 70 and 96 K are presented here. After each isotherm was measured the sample cell was warmed to room temperature and evacuated for at least 12 h.

Figure 2 shows a subset of the adsorption isotherms taken between 70 and 96 K, more than fifty isotherms were recorded in steps of about 0.5 K. Remarkably, we observed at least five isotherm steps of nearly equal height over the entire range studied, leading us to believe that the molecular density of the layers is rather uniform with no large variation in the adsorption potential nor particle size throughout the powder.

We examined how the reported sensitivity of MgO to moisture and its known chemical reactivity affects a sample's quality and the reproducibility of the isotherm, using

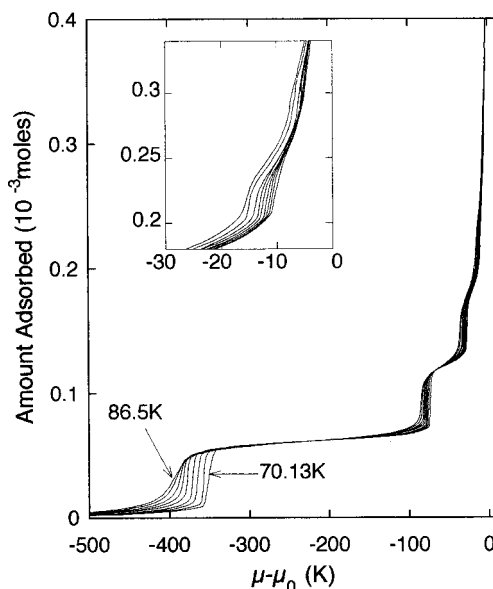


FIG. 2. Set of isotherms (chemical potential versus coverage) for temperatures between 70 and 96 K.

three different MgO samples and measuring several isotherms at the same temperature (usually near the beginning and end of a run of several weeks). We were especially concerned about the sample's degradation during long experimental runs (i.e., 3–4 weeks). In one set, consecutive isotherms were measured while increasing the temperature, in another set consecutive isotherms were recorded while decreasing the temperature, and for a third sample, the temperature was varied randomly for consecutive isotherms. There was no evidence suggesting that the sequence followed was important. Some minor degradation of the sample was apparent after runs longer than 3–4 weeks.

III. RESULTS AND DISCUSSION

Because several different MgO samples were used during this investigation we minimized random and systematic errors by processing the isotherm data in the following way. First, the experimental data from each isotherm was fitted with a smooth curve using the interpolation function of a commercial software package (Kaleidagraph®). This routine uses an algorithm that generates a smooth curve passing through each data point unless there is a discontinuity in the slope at one of them.¹⁷ For each isotherm, we typically recorded between 200 and 300 data points. Figure 3 illustrates how accurately the interpolation procedure reproduces our data.

We subsequently used the interpolated curves to extract the thermodynamic quantities. For example, the numerical derivative of each isotherm can be used to precisely locate the position of each adsorption step. The location of these pressure steps associated with the formation of the *n*th layer can be plotted as a function of inverse temperature and fit to the Clapeyron equation:

$$\log_{10}(p^{(n)}[\text{torr}]) = B^{(n)} + A^{(n)}/T. \quad (1)$$

Figure 4 shows a linear fit to Eq. (1) using both the logarithm of the saturated vapor-pressure bulk of bulk methane, p_0 ,

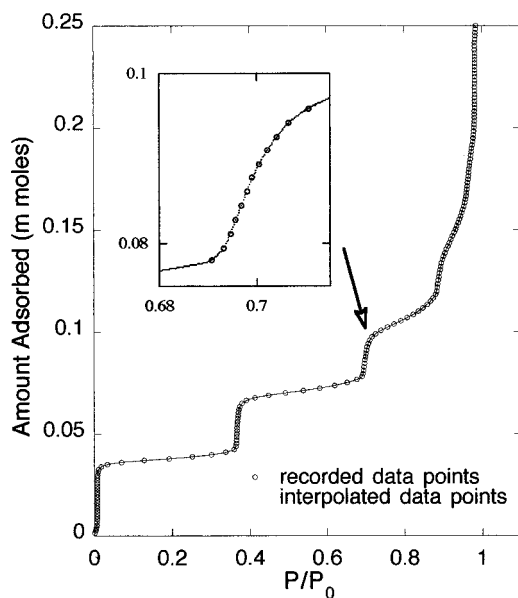


FIG. 3. Data points recorded and interpolation (solid curve) for an isotherm taken at 74.34 K (reduced pressure versus coverage). The inset shows a detail from the third adsorption step of this isotherm.

and the logarithmic pressure location of each adsorption step $p^{(n)}$ as function of inverse temperature. From these fits the coefficients $A^{(n)}$ and $B^{(n)}$ were determined (see Table I); several observations can be made about them. First, the coefficients $A^{(n)}$ indicate that at lower temperatures, it is increasingly difficult to differentiate between films that are four or five layers thick and the bulk methane. Extrapolating the fits for $p^{(4)}$ and $p^{(5)}$ with the fit for p_0 , shows that at a temperature of 48.0 ± 2 K the $p^{(5)}$ curve intersects with the

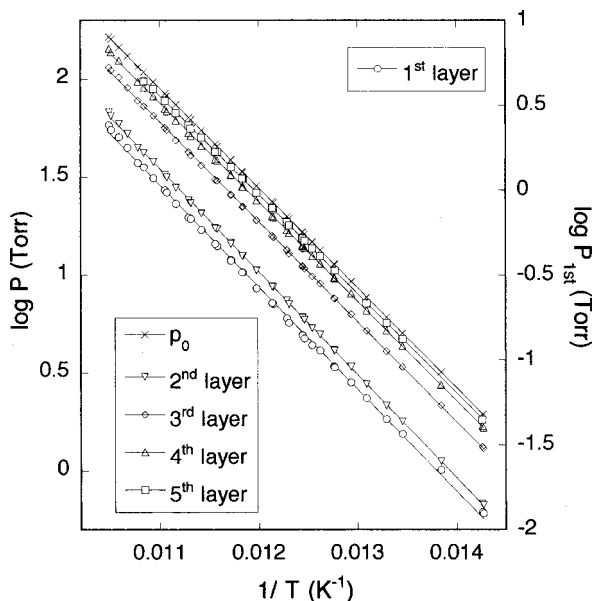


FIG. 4. $\log_{10}(P[\text{torr}])$ of adsorption steps 1 through 5 and of the saturation vapor pressure p_0 plotted as function of inverse temperature. For the fifth adsorption step, only data points are included for which the adsorption step was clearly observed. The parameters for the fit of the Clapeyron equation (solid line) to the data is summarized in Table I.

p_0 curve, while $p^{(4)}$ intersects it at 26.4 ± 2 . Unfortunately, at these temperatures, the saturated vapor pressure of methane is too low to measure isotherms. However, Larese and co-workers found at low temperatures when the coverage of methane on MgO exceeds four or five layers, the rotational tunneling spectra converge towards that observed for bulk methane.⁵

Adsorption isotherms also can be used to characterize the response of the methane film to a change in spreading pressure by calculating the 2D compressibility, K_{2D} :

$$K_{2D} = (A^*p)/(N_A^*k_B^*T^*N^2)^*dN/dp, \quad (2)$$

where A is the surface area of the substrate, p the pressure, N_A Avogadro's number, k_B Boltzmann's constant, and N the number of adsorbed molecules. Larher and Angerand demonstrated¹⁸ that the 2D compressibility is an extremely useful quantity for tracking thermodynamic changes in the adsorbed film and identifying the location of phase transitions. They found that both the intensity and width of the compressibility as function of chemical potential provides important information about changes in the structural properties of the layers. Based on his findings, it is generally accepted that narrow (broad) compressibility peaks are usually associated with solid (liquid) layers. Thus, monitoring the width of the compressibility peak as function of temperature is useful for locating a melting transition.

We did not produce a functional form for the shape of the compressibility peaks since there were several parameters that we could not properly characterize (e.g., the size distribution and heterogeneity of the MgO powder sample, and the instrument's response function). Therefore, we used the full-width-at-the-half-maximum (FWHM) of the compressibility peak (regardless of its shape) to track the behavior of compressibility with temperature.

Figure 5 shows the compressibility derived from the isotherms displayed in Fig. 2 as function of chemical potential for the first and second adsorption steps. Its peak is largest for the monolayer films and decreases as subsequent layers are added. Since the strength of the molecule-substrate interaction decreases with increasing film thickness, it is not surprising that the magnitude of the compressibility decreases as the number of methane layers on the substrate increases. For example, the mean value of the bilayer compressibility peak is about a factor of 5 smaller than the mean monolayer value. Furthermore, since temperature-driven phase transitions take place, it also is not unusual that changes are observed in the magnitude of the compressibility peak as a function of temperature. For example, at monolayer thickness, the compressibility peak decreases by a factor of about 20 over an interval of a few degrees.

Not only are there changes in the magnitude of the compressibility, but changes in the width also are observed. To illustrate the changes in the FWHM of the compressibility as function of temperature, Figs. 6(a) and 6(b) display the behavior for layer 1, and layers 2 through 4, respectively. Figure 6(a) clearly shows that the width of the monolayer compressibility feature is nearly constant up to 80 K, above which it broadens dramatically, indicating that a phase transition takes place near 80 K. Most likely, the change in width is due to a transformation from a high-density phase (solid-like) to a lower density (liquidlike) phase. This observation

TABLE I. Thermodynamic quantities for the CH₄/MgO system calculated from the isotherm measurements.

	1st layer	2nd layer	3rd layer	4th layer
$A^{(n)}$	601.59 ± 3.017	526.2 ± 1.06	510.75 ± 1.06	507.08 ± 0.818
	690.3 ± 22.6 ^a	529.4 ± 2.6 ^a	511.3 ± 5.3 ^a	506.6 ^a
$B^{(n)}$	6.6477 ± 0.036	7.3309 ± 0.0128	7.4002 ± 0.0128	7.4569 ± 0.0093
	7.676 ± 0.25 ^a	7.385 ± 0.031 ^a	7.42 ± 0.064 ^a	7.462 ^a
$T_{cr}(K)$	80 ± 0.5	85 ± 1	85 ± 1	85 ± 1
	80 ± 2 ^a	≥ 87 ^a	≥ 87 ^a	
$K_{2D}(mm/N)$	1.5 × 10 ⁷	2 × 10 ⁶	7 × 10 ⁵	4 × 10 ⁵
[$T < T_{cr}$]				
$K_{2D}(mm/N)$	1.3 × 10 ⁶	1 × 10 ⁶	3 × 10 ⁵	2 × 10 ⁵
[$T > T_{cr}$]				
$Q_{st}(KJ/mol)$	14.4 ± 2 [89.1]	10.4 ± 1 [82.7]	9.94 ± 1 [83.46]	9.85 ± 1 [83.46]
[$T(K)$]	13.22[89.1] ^a	10.12[82.7] ^a	9.79[82.7] ^a	9.71[82] ^a

^aData from Ref. 12.

agrees well with the monolayer melting temperature of 80 ± 2 K reported earlier by Coulomb *et al.*³ and Gay, Suzanne, and Coulomb. We note that the data in Fig. 6 are derived from three different samples, each with a slightly different surface area. The temperature at which the phase transition occurs is independent of the sample used, however, the temperature dependence of the width of the compressibility feature above the phase transition is slightly dependent on the surface area of the substrate. The sample with the largest surface area, that is about twice the surface-to-volume ratio compared to the smallest sample, exhibits a slightly greater slope. Further, we note that as the surface-to-volume ratio of the powder increases (i.e., smaller MgO crystallites), the compressibility of the film decreases slightly, probably because the edges of the MgO crystallites play a fractionally greater role in determining the stability of the films, thereby increasing the width of the compressibility peak. Figure 6(b) shows that the compressibility for films, two-to-four layers thick, is nearly independent of temperature regardless of the

initial film's thickness below the phase transition. While the data is more scattered at higher temperatures, we can establish with some certainty that the phase-transition temperature for layers 2 through 4 is 85 ± 1 K. Earlier reports indicated that the phase-transition temperatures for the second and third layers were ≥ 87 K. Finally, Table I summarizes the mean values of the 2D compressibility of the CH₄ film above (low density) and below (high density) the phase transition. For the monolayer film, these values differ by about an order of magnitude while for layers 2–4 they differ by about a factor of 2.

Another important thermodynamic quantity related to layer growth of an adsorbate on a substrate is the isosteric heat of adsorption. It is defined as the energy necessary to bring a particle from infinity onto the surface (clean or pre-dosed with gas). The isosteric heat of adsorption can be calculated thus at constant coverage:

$$Q_{st} = RT^2 \partial(\ln p) / \partial T. \quad (3)$$

We approximated the partial derivative in Eq. (3) by calculating $\Delta(\ln p) / \Delta T$ at constant coverage from two adjacent isotherms separated by a temperature difference of about 1 or 2 K. The numerical value of the isosteric heat calculated in this way is weakly dependent on the temperature interval. As the temperature interval is decreased the value obtained for the isosteric heat should converge towards the real differential (i.e., become more accurate). However, not only does the temperature interval chosen effect the value of Q_{st} , but some extrapolation is required to produce the isosteric data since all of the isotherms are not measured at exactly the same coverage. Both these uncertainties contribute to the accuracy with which Q_{st} can be determined. However, because all of the data reduction was performed consistently, we believe that the variation of Q_{st} with coverage and temperature is accurately represented.

Figure 7 shows the variation of Q_{st} as a function of surface coverage for several temperatures near 80 K. The temperature interval used in calculating Q_{st} is approximately constant (i.e., about 2 ± 0.1 K). Several comments can be made about the behavior of the Q_{st} . First, a peak in the heat of adsorption is readily observable for the first, second, and

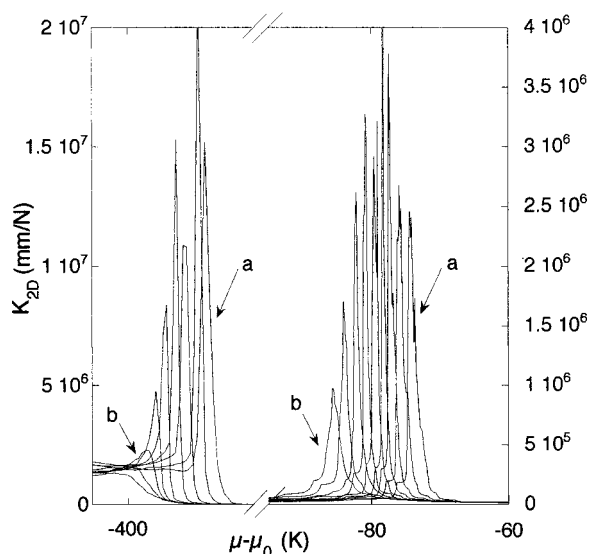


FIG. 5. Compressibility versus chemical potential of set of isotherms between 70 K (a) and 86 K (b) for the first and second adsorption step.

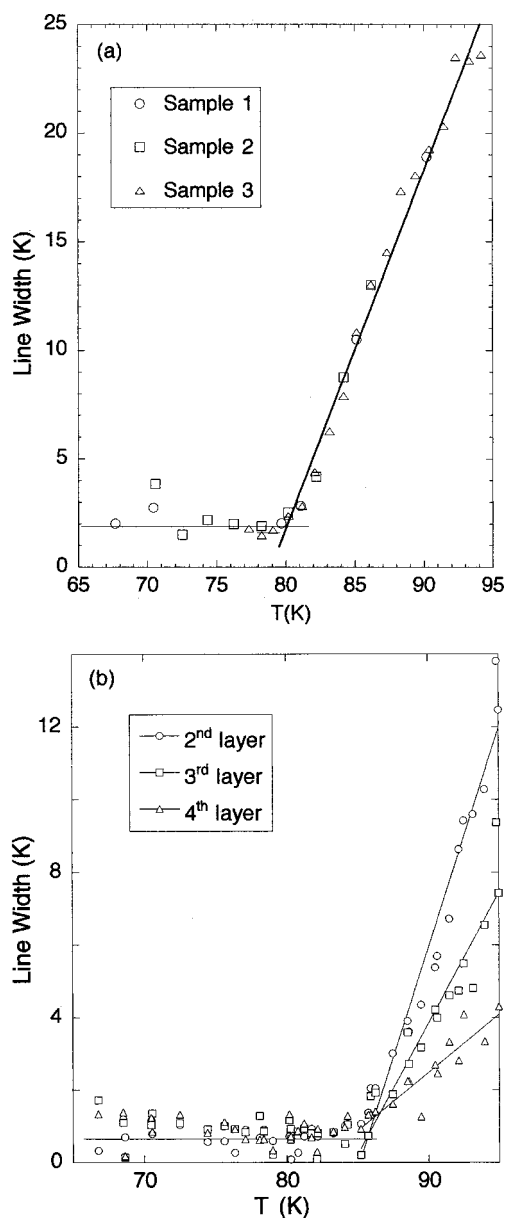


FIG. 6. The linewidth of the compressibility peak of layers 1 through 4 is plotted versus temperature. A linear fit of the sloping part of the data gave a transition temperature of about 80 K for the (a) monolayer and of about 85 K for (b) layers 2 through 4. Transition temperatures and error are summarized in Table I.

even possibly the third layers. The magnitude of Q_{st} is greatest at monolayer coverage, and peaks near the completion of the monolayer. It is still easy to identify the relative maximum in Q_{st} near the completion of the bilayer; however, this relative maximum is less obvious for layers three and above. Furthermore, the variation in Q_{st} decreases as the film thickness increases. These observations are consistent with the fact that as the film grows thicker on the substrate, a methane molecule that joins the film from the vapor experiences a force dominated by molecule-molecule interaction and not the molecule-substrate interaction. Furthermore, regardless of the status of the film, the fall off from the peak in Q_{st} at the completion of a layer is indicative of the layer's relative stability. Finally, the isosteric heat is roughly constant (~ 9.75 kJ/mol) for coverages of more than 5 layers. We note

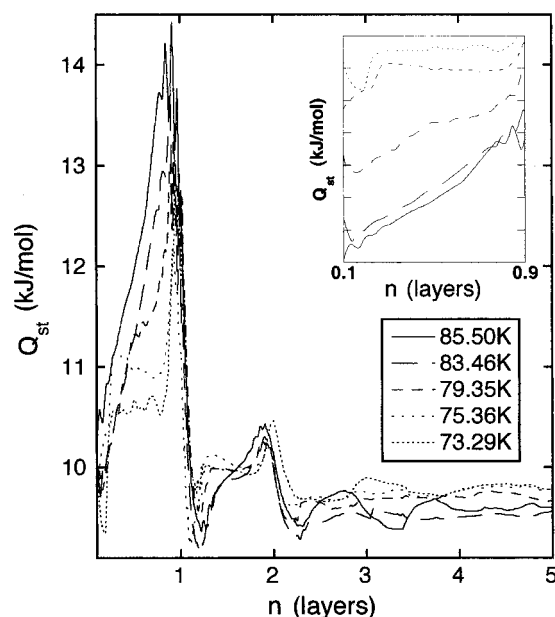


FIG. 7. Isosteric heat of adsorption Q_{st} versus reduced coverage for a set of isotherms at temperatures between 73.29 and 85.5 K. The inset shows the shape of isosteric heat curves for the first adsorption step. These curves are offset by a small amount to display the progression with temperature. The temperature increases from top to bottom.

that this value is still quite different from the latent heat of vaporization of bulk methane [~ 8.68 kJ/mol at 91 K (Ref. 19)]. The difference in Q_{st} is most likely due to the effect of the MgO substrate on the 4–5-layer film, and also perhaps because the methane film grows like the (100) face of bulk CH_4 on the MgO substrate. Some limited data are available for comparison with our values for Q_{st} . Table I shows how the peak values of Q_{st} we determined compare with earlier measurements as a function of coverage. An alternative approach for calculating Q_{st} , described by Madih,¹² uses the Clapeyron coefficient $A^{(n)}$. With these data, we derive similar values for Q_{st} for layers 1–4 as were measured, ranging from 13.221 through 9.707 kJ/mol.

Below 80 K (i.e., below the phase transition identified using the compressibility), there is a rapid and nominally linear increase in Q_{st} between 0–0.2 layers. This behavior can be understood in the following way. At low coverage, the methane film forms as a dilute, lattice gas on the surface of MgO. As the density of the lattice gas increases, the likelihood of near-neighbor interactions rises resulting in the observed increase in Q_{st} . Between 0.2 and ~ 0.9 layers, Q_{st} is nearly constant, presumably reflecting the formation of islands of a commensurate $\sqrt{2} \times \sqrt{2} R45^\circ$ solid. Finally, near the completion of the layer, the rapid increase with coverage of Q_{st} is most likely due to a slight film compression, the interactions between solid domains and the crossing of domain walls. The same description can be applied to the changes in Q_{st} observed over the same relative coverage range for the bilayer below ~ 85 K. It is also applicable for higher layers as long as layer-by-layer growth occurs and a sharp interlayer interface is retained. At temperatures > 80 K for the monolayer and > 85 K for the bilayer, fluidlike methane layers form. Increasing the methane coverage entails an attendant increase in density and near-neighbor interaction

causing a steady increase in Q_{st} . This behavior is consistent with our earlier suggestions that a phase-transition occurs, signaled by the dramatic change in width of the compressibility as a function of temperature [see Figs. 6(a) and 6(b)]. Furthermore the formation of a fluidlike phase at these temperatures and coverages is in agreement with earlier neutron-scattering results.^{2,6,15,16}

While the absolute value of Q_{st} shows no clear temperature dependence, we note that the difference ΔQ_{st} (without considering of the shape of the peak and noise) increases as the temperature increases, as expected.

IV. CONCLUSIONS

We derived several thermodynamic properties of the CH_4/MgO system from our isotherm measurements. The 2D compressibility for various films of CH_4 on MgO films was determined. A phase transition between a solidlike and fluidlike phase was identified for the first through fourth layer. We found that these take place at 80 ± 0.5 K for the first layer

and 85 ± 1 K for second through fourth layers. These results place tighter bounds on the location of the phase transformations than previous results.

The isosteric heat of adsorption as function of coverage was used to gain additional insight into the layer-by-layer growth of the methane film on MgO. We believe that our results will aid in refining models for the interaction of methane with MgO(100) surfaces, and expect that such improvements in the intermolecular potentials will be useful in rendering accurate computer simulations of this molecular adsorption system.

ACKNOWLEDGMENTS

The authors would like to thank our colleagues Michael Sprung, Julius Hastings, Colin Carlile, and Walter Kunnmann for useful discussions as well as C. Koehler III for his excellent technical assistance. This work was supported by the U.S. Department of Energy, Materials Science Division under Contract No. DE-AC02-98CH10886.

¹L. W. Bruch, M. W. Cole, and E. Zaremba, *Physical Adsorption: Forces and Phenomena* (Oxford University, Oxford, 1997), and references therein.

²J. P. Coulomb, T. S. Sullivan, and O. E. Vilches, *Phys. Rev. B* **30**, 4753 (1984).

³J. P. Coulomb, K. Madih, B. Croset, and H. J. Lauter, *Phys. Rev. Lett.* **54**, 1536 (1985).

⁴J. M. Gay, J. Suzanne, and J. P. Coulomb, *Phys. Rev. B* **41**, 11 346 (1990).

⁵J. Z. Larese, *Physica B* **248**, 297 (1998).

⁶A. Lakhlifi and C. Girardat, *Surf. Sci.* **241**, 400 (1991).

⁷J. M. Gay, P. Stocker, D. Degenhardt, and H. J. Lauter, *Phys. Rev. B* **46**, 1195 (1992).

⁸D. R. Jung, J. Cui, and D. R. Frankl, *Phys. Rev. B* **43**, 10 042 (1991).

⁹B. Deprick and A. Julg, *New J. Chem.* **11**, 299 (1987).

¹⁰S. Picaud, C. Girardet, T. Duboo, and D. Lemoine, *Phys. Rev. B*

60, 8333 (1999).

¹¹K. Todnem, K. J. Borve, and M. Nygren, *Surf. Sci.* **421**, 296 (1999).

¹²K. Madih, Thesis, Université d'Aix-Marseille, Marseille, 1986.

¹³J. Z. Larese, B. Asmussen, M. A. Adams, C. Carlile, D. Martin, and M. Ferrand, *Physica B* **226**, 221 (1996).

¹⁴J. Z. Larese, J. M. Hastings, L. Passell, D. Smith, and D. Richter, *J. Chem. Phys.* **95**, 6997 (1991).

¹⁵W. Kunnmann and J. Z. Larese (unpublished).

¹⁶Z. Mursic, M. Y. M. Lee, D. E. Johnson, and J. Z. Larese, *Rev. Sci. Instrum.* **67**, 1886 (1996).

¹⁷R. W. Stineman, *Creative Comput.* **6**, 54 (1980).

¹⁸Y. Larher and F. Angerand, *Europhys. Lett.* **7**, 447 (1988).

¹⁹V. V. Sychev, A. A. Vasserman, V. A. Zagoruchenko, A. D. Kozlov, G. A. Spiridonov, and V. A. Tsymarny, *Thermodynamic Properties of Methane* (Hemisphere Publishing Corp, New York, 1987).